First principle based computations to evaluate propane and butane detection capabilities of gold doped graphene based gas sensor devices

Indranil Maity[1*], *Souvik* Bhanja[2]

[1]Associate Professor, Department of Electronics & Communication Engineering, Institute of Engineering and Management (IEM), University of Engineering and Management (UEM), Kolkata, West Bengal, India
[2]Student, Department of Electronics & Communication Engineering, Institute of Engineering and Management (IEM), Kolkata, West Bengal, India

Abstract. The present study focuses on the performance of gold (Au) doped graphene sheet in the presence of liquefied petroleum gas (LPG) molecules viz. propane and butane using first principle-based calculations, and all the results were compared via investigating different electronic and molecular properties. The propane and butane adsorbed Au-doped graphene-based structures were optimized using Gaussian 09W and GaussView 6.0 software tools. In the current attempt, the following electronic and gas-sensing parameters were studied including FMO (Frontier Molecular Orbitals) i.e., HOMO (Highest Occupied Molecular Orbital)-LUMO (Lowest Unoccupied Molecular Orbital), MEP (Molecular Electrostatic Potential) map, Raman spectra, FTIR (Fourier Transform Infrared Spectroscopy), I-V characteristics, adsorption energy, and binding distance. The HOMO-LUMO gap was found to be larger in the case of propane-adsorbed Au-doped graphene. MEP study also helps to visualize the interaction site and the underlying electronic characteristics. Similarly, adsorption energies and binding distances were calculated and used as key parameters for comparing the gas sensing performance. It was observed that the adsorption energy of propane on Au-doped graphene sheet was 1.159 times higher than that of butane, which indicates better detection capabilities of the sensing material (Au-doped graphene) towards propane among the other constituents of the LPG molecules.

1 Introduction

Liquefied petroleum gas (LPG) is one of the major energy sources consumed globally, primarily consisting of hydrocarbons like propane (C_3H_7) and butane (C_4H_{10}). LPG is widely used as a fuel in various sectors, such as domestic heating and cooking, industrial applications, and as a vehicular fuel [1]. LPG has a higher calorific value, and it is more convenient to store and transport, which are significant reasons for its popularity as a fuel.

* Corresponding author : indrasanu026@gmail.com

Although LPG has numerous benefits, it is also highly flammable and dangerous. Leaked LPG can lead to disastrous fires and explosions as well as severe health issues such as dizziness and unconsciousness. Thus, the development of reliable and efficient LPG detection systems has become an important challenge for researchers. Advanced sensors with high sensitivity and selectivity for the detection of major LPG components, such as propane and butane, are instrumental in preventing accidents and ensuring safety in both residential and industrial areas [2-3].

Gas sensor technology has improved in recent years with applications in diverse fields to ensure safety and environmental monitoring. Graphene, a 2D nanomaterial with high carrier mobility and superior electrical and thermal conductivity, is a promising candidate for various electronic and sensing applications. Though pristine graphene has many advantages, it has several drawbacks, such as zero band gap, and the surface area is not optimum for efficient adsorption of gases [4-6]. This limits its effectiveness as a high-performance gas sensor. These challenges of pristine graphene can be addressed through doping with transition metals, which has become an efficient approach. Doping increases the number of active sites on the material surface that interact with the gas molecules. In this work, pure graphene was doped with Au atoms to enhance its gas-sensing ability. The catalytic properties of Au enhance both chemical and electronic sensitization, thus improving the overall sensing performance [5].

A room temperature-based LPG sensor was developed by Amarnath et al. utilizing $CoSnO_2$ nano islands deposited graphene layers to evaluate its sensitivity [1]. Singh et al. discussed the room temperature detection of LPG gases by incorporating sulfur-doped silicon carbide nanotube as a sensing material [3]. Singla et al. studied the hydrogen gas adsorption behaviour of nitrogen, boron, and Au co-doped graphene [5]. However, a detailed analysis of LPG detection using doped-graphene-based gas sensors remains unexplored.

This paper gives a comprehensive analysis of the behaviour of Au-doped graphene sheet towards the detection of propane and butane gases. All the key parameters such as HOMO-LUMO gap, molecular electrostatic potential (MEP), Raman spectra, FTIR spectra, and I-V characteristics were computed to understand the sensing mechanisms at the molecular level. Additionally, the adsorption energy was calculated, and the results were systematically compared to thoroughly assess the sensing behaviour of the material. Response magnitude and recovery time were also computed to determine the practical feasibility of our proposed gas sensor. Based on the available literature, no previous work has provided a detailed comparative analysis of propane and butane sensing capabilities or performed first-principles optimization of Au-doped graphene sheets using Gaussian and GaussView software. This work fills this research gap by offering new insight into the possibility of gold-doped graphene as an efficient gas-sensing material for LPG detection.

2 Computational Details

In this study, first principles based calculations were performed to optimize the Au-doped graphene structure. The Au atom was placed on the surface of the monolayer graphene structure by replacing one carbon atom position (i.e., the designed structure had one carbon vacancy). Both the structures consist of 29 carbon atoms, 14 hydrogen atoms, and 1 gold atom as shown in Fig. 1. The sensing material was geometrically optimized in the presence of propane and butane using Gaussian 09W and GaussView 6.0 simulation platform. For optimization, first principle based semiempirical methods were implemented along with PM6 functional. As both systems consisted of an odd no of electrons, the unrestricted method was

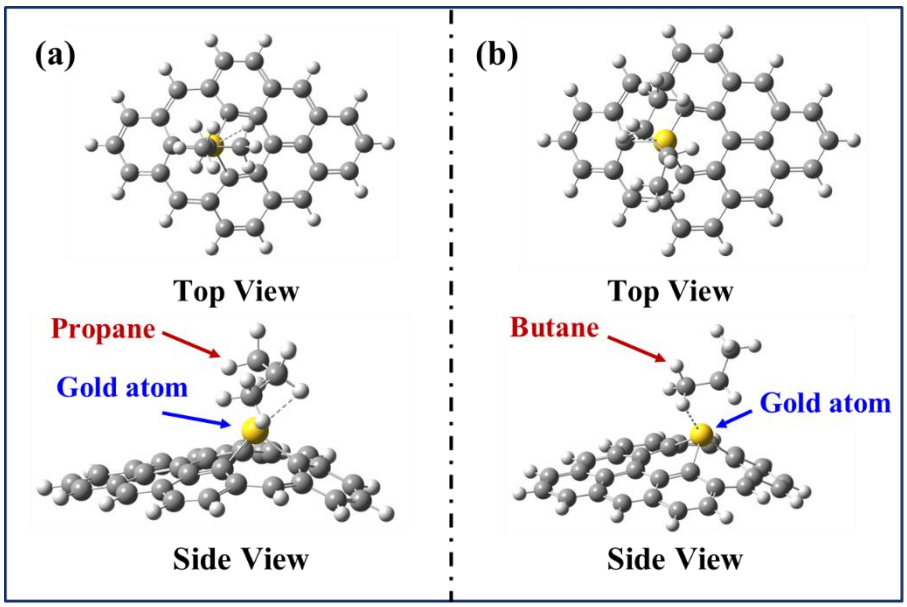

Fig. 1. Optimized structure of (a) propane adsorbed Au-doped graphene sheet, and (b) butane adsorbed Au-doped graphene sheet

selected for the calculations. Additionally, SCF=XQC keyword was chosen to set the convergence criteria in order to obtain the fully optimized structure. The current-voltage characteristics of Ag-doped graphene-based device have been calculated using DFTB+ software under the Materials studio package utilizing the Slater-Koster library named "Au-org". FTIR and Raman spectra were obtained from frequency calculation in the Gaussian 09W software platform. Origin 2025b software was employed for the plotting of FTIR spectra and I-V characteristics. The adsorption energy was derived using the following formula:

$$E_{Ads} = E_{Sensor+gas} - (E_{gas} + E_{sensor}) \quad (1)$$

where, E_{Ads} signifies the adsorption energy of the overall system, E_{gas} signifies the electronic energy of the adsorbate gas, E_{sensor} indicates the electronic energy of the sensor and $E_{Sensor+gas}$ denotes the electronic energy of the sensing material with gas, respectively. The sensitivity of the proposed gas-sensor device was calculated using the following equation: $S = \frac{\sigma_S - \sigma_{S+G}}{\sigma_S} \times 100$ (2)

where, σ_S and σ_{S+G} are the conductivity of the sensing material and the gas-adsorbed sensing material, respectively. The conductivity of the structure was calculated based on the HOMO-LUMO energy gap using the equation:

$$\sigma = \sigma_0 e^{-\left(\frac{E_g}{2kT}\right)} \quad (3)$$

where, σ is the conductivity, σ_0 is the proportionality constant, E_g is the HOMO-LUMO energy gap and k is the Boltzmann's constant. Furthermore, Recovery time, which is an essential gas-sensing parameter can be expressed as:

$$\tau = \upsilon^{-1} e^{-\left(\frac{E_{ad}}{kT}\right)} \quad (4)$$

where, τ is the recovery time, υ^{-1} is the attempt frequency, which is typically $10^{12}s^{-1}$, E_{ad} is the adsorption energy and k is the Boltzmann's constant and T is the room temperature (300K) [3][7].

3 Results and Discussion

3.1 HOMO-LUMO Analysis

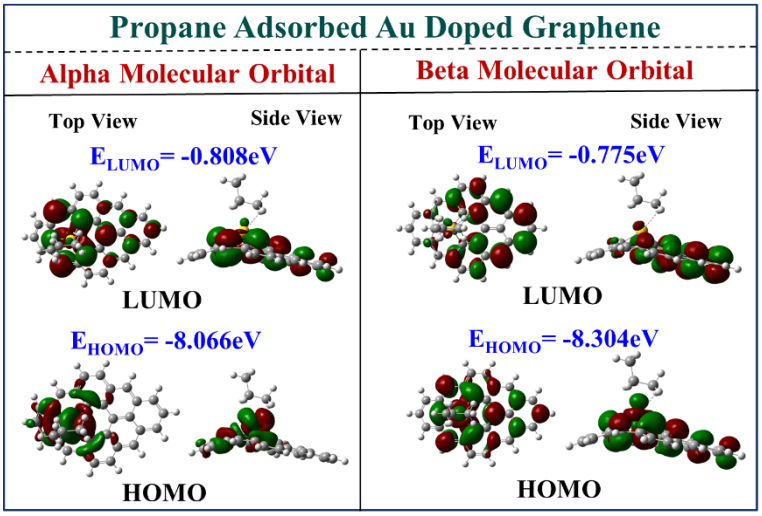

Fig. 2. Alpha and Beta molecular orbital of propane adsorbed Au-doped graphene structure

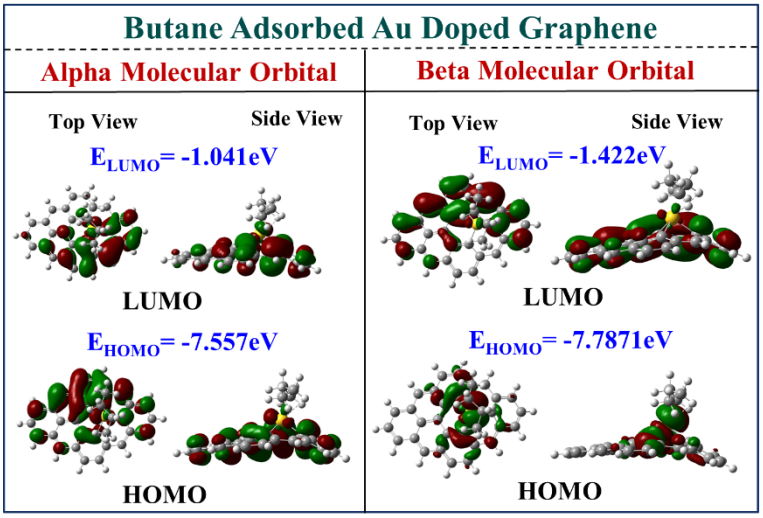

Fig. 3. Alpha and Beta molecular orbital of butane adsorbed Au-doped graphene structure

HOMO-LUMO orbitals, also known as frontier molecular orbitals (FMOs), are essential for understanding the electronic and chemical behaviour of a molecular system. Fig. 2 and Fig. 3 depict the HOMO-LUMO orbitals of the propane-adsorbed Au-doped graphene sheet, and the butane-adsorbed Au-doped graphene sheet, respectively, with an isovalue of 0.02. Due to the presence of an odd number of electrons in both systems, both alpha orbitals (up-spin electrons) and beta orbitals (down-spin electrons) were generated. The red and green regions in the HOMO-LUMO isosurface denote positive and negative electron densities, respectively [8]. Higher density of HOMO and LUMO orbitals indicates the electron-donating and electron-accepting properties, respectively. The HOMO-LUMO gap ($E_{HOMO–LUMO}$ gap)

serves as a vital parameter for determining molecular stability and chemical reactivity. From Table 1, it is observed that the propane adsorbed Au-doped graphene structure has a larger HOMO-LUMO gap compared to butane, which highlights the fact that propane-adsorbed structure has more stability and thus it has lesser chemical reactivity [9].

Table 1. Molecular orbitals with their corresponding energy values for the two examined systems

Au-doped graphene sheet with propane (case 1)			**Au-doped graphene sheet with butane (case 2)**		
Parameters	**For Alpha orbital**	**For Beta orbital**	Parameters	**For Alpha orbital**	**For Beta orbital**
E_{HOMO} (eV)	-8.066	-8.304	E_{HOMO} (eV)	-7.557	-7.871
E_{LUMO} (eV)	-0.808	-0.775	E_{LUMO} (eV)	-1.041	-1.422
$E_{HOMO-LUMO\ gap}$ (eV)	7.258	7.529	$E_{HOMO-LUMO\ gap}$ (eV)	6.516	6.449

3.2 Molecular Electrostatic Potential (MEP) Analysis

MEP is a valuable property in molecular studies that can offer significant information about molecular structures and their physiochemical properties through 3D visualization [9]. The study of MEP is useful for analyzing the relationship between molecular structure and reactivity and is beneficial for drug, biomolecule, and chemical studies. MEP directly correlates with electron density, with the red region on the 3D map portraying high electron density, and the blue region denoting a lower number of electrons. The electrostatic potential increases from the red region to the blue region, which is shown in Fig. 4 using different colour mapping. To plot the MEP map, the colour legend was set between -1.106e1 and -7.125e0, ranging from red region to blue region. The red regions in both Fig. 4(a) and Fig. 4(b) were mainly formed near the adsorption site of the gas and the sensing material indicating more number of electrons in those regions, which increases the possibility for

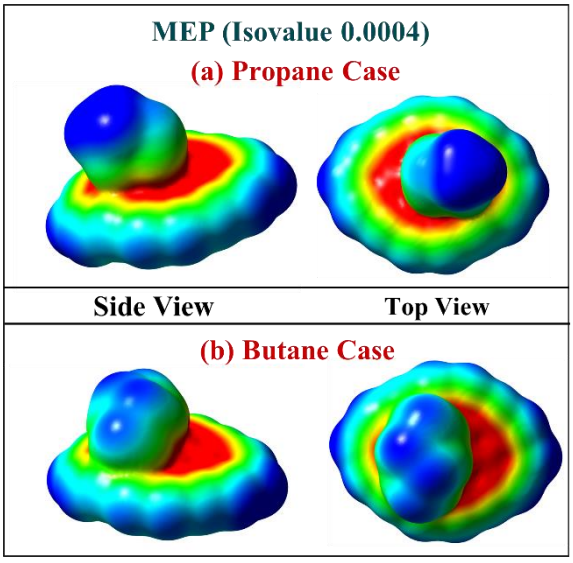

Fig. 4. Molecular electrostatic potential of (a) propane adsorbed, and (b) butane adsorbed Au-doped graphene structure

electrophilic attack in those regions. The green portion, which surrounded the red region in both the figures indicates neutral region. The blue region was more prominent in the hydrogen-passivated site of the Au-doped graphene sheet, and top portions of the adsorbate gas/vapour, which implies less number of electrons making that zone more suitable for a nucleophilic attack [9-10].

3.3 Raman Spectrum

The vibrational characteristics of Au-doped graphene upon adsorption of propane and butane are shown in Fig. 5. Both Raman spectra exhibited prominent peaks corresponding to the characteristic bands of graphene, including the D-band (centred at 1357 cm^{-1} for propane and 1356 cm^{-1} for butane), G-band (centred at 1562 cm^{-1} for propane and 1572 cm^{-1} for butane), and 2D-band (centred at 2758 cm^{-1} for propane and 2757 cm^{-1} for butane). The D-band signifies defects in the sensing material, while the G-band is associated with the in-plane stretching of the sp^2 carbon bonds. The 2D-band, a second-order overtone of the D-band, reflects the layers of the graphene structure [11]. In propane-adsorbed Au-doped graphene, the Raman peaks show moderate shifts and variations in intensity, indicating a certain level of interaction between the gas molecule and the Au-doped graphene surface. In contrast, butane adsorption results also showed intensity variation, suggesting a possible charge transfer effect between the gas and the adsorbent. The differences in spectral modifications between propane and butane adsorption highlight the selectivity of Au-doped graphene towards different hydrocarbon gases, highlighting its applicability in advanced gas sensors.

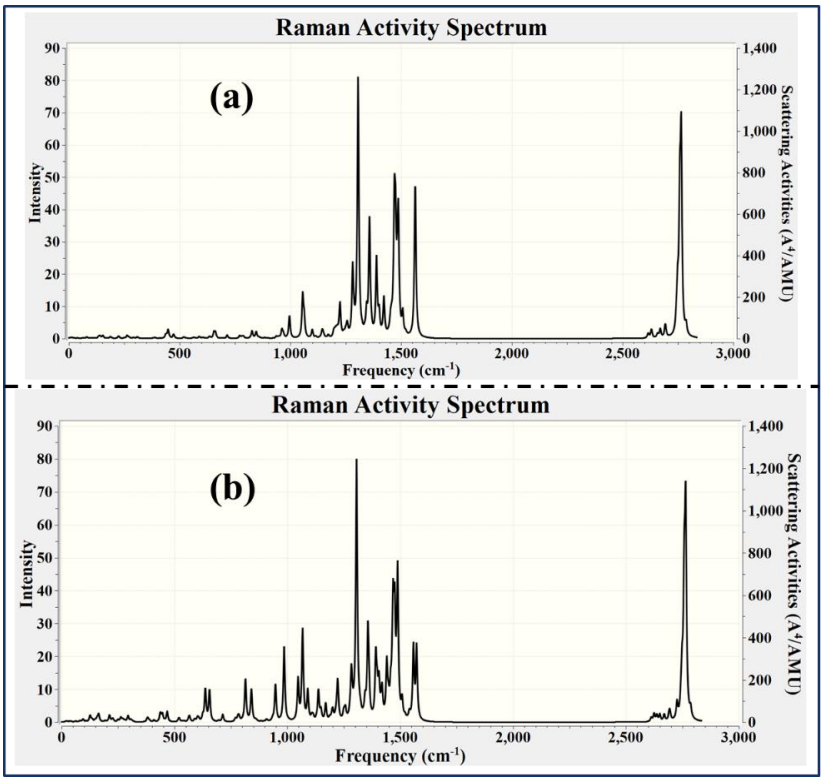

Fig. 5. Raman spectra of (a) propane adsorbed, and (b) butane adsorbed Au-doped graphene structure

3.4 FTIR Spectroscopy

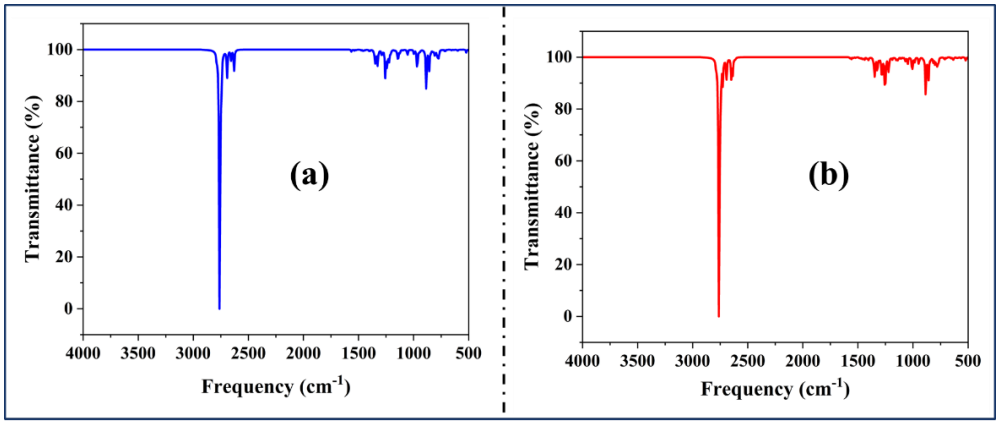

Fig. 6. FTIR spectroscopy of (a) propane adsorbed, and (b) butane adsorbed Au-doped graphene structure

The FTIR spectroscopy results illustrate the vibrational characteristics of Au-doped graphene during gas adsorption. In Fig. 6(a), where propane is adsorbed onto the Au-doped graphene structure, a prominent absorption peak was observed around 2893 cm^{-1}, corresponding to the C-H stretching vibrations of propane molecules [12]. Additional peaks in the fingerprint region (500-1500 cm^{-1}) indicate the presence of bonding or structural changes due to gas adsorption. Similarly, in Fig. 6(b), where butane is adsorbed, a strong absorption band appears near 2800 cm^{-1}, attributed to the C-H stretching vibrations of butane. The spectral variations between propane and butane adsorption showed distinct molecular characteristics between the gas and the Au-doped graphene.

3.5 I-V Characteristics

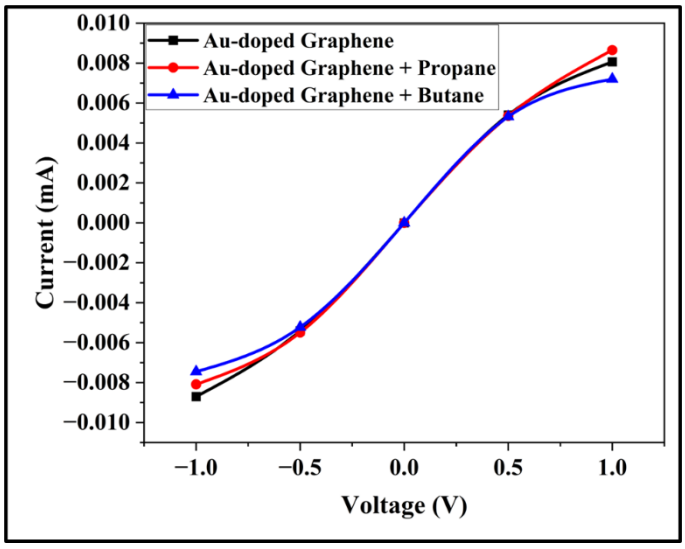

Fig. 7. I-V characteristics of (a) propane adsorbed, and (b) butane adsorbed Au-doped graphene structure

The current-voltage characteristics of Au-doped graphene under three different conditions i.e., pristine, propane-adsorbed, and butane-adsorbed are shown in Fig. 7. The curve for pure Au-doped graphene exhibited a non-linear trend indicative of semiconductor-like behaviour [4][13]. In the case of propane adsorption, a slight shift in the current was observed, particularly at negative voltages (-0.008 mA), suggesting charge transfer and measurable adsorption between the propane and Au-doped graphene. In contrast, the butane adsorption result showed an I-V curve nearly identical to the pristine case. Propane-adsorbed Au-doped graphene (red curve) showed a higher current response than butane-adsorbed Au-doped graphene (blue curve) at higher voltages. These observations highlight the sensitivity of Au-doped graphene since it exhibits a more pronounced response to propane compared to butane. This makes Au-doped graphene a promising candidate for propane gas sensing applications [6][13].

3.6 Sensitivity, Conductivity and Recovery Time Study

Different real-time gas sensing metrics were obtained to validate the simulated results with practical observations. Sensitivity is an important parameter that directly correlates with the adsorption energy and the charge transfer between the adsorbate and the adsorbent. Similarly, conductivity primarily depends on the variation of the HOMO-LUMO energy gap of the system. Recovery time indicates the reusability of a gas sensor which depends upon the adsorption energy and operating temperature. Higher negative adsorption energy leads to chemisorption; resulting in a prolonged recovery time. These three real-time gas sensing parameters are calculated and compared in Table 2 [7].

Table 2. Electronic conductivity ratio, sensitivity and recovery time of propane and butane adsorbed Au-doped graphene sheet

System	**Electronic conductivity ratio** $(\mathbf{ln}\frac{\sigma_0}{\sigma})$	**Sensitivity (%)** (S)	**Recovery Time (ps)** (τ)
Propane with Au-doped graphene	139.57	99.64	8.73E+17
Butane with Au-doped graphene	125.23	98.72	2.96E+15

3.7 Adsorption Energy and Binding Distance

Adsorption energy and binding distance are the two major gas sensing parameters from the perspective of gas adsorption. Negative adsorption energy signifies feasible adsorption, whereas, positive adsorption energy implies that the adsorption process is unfavorable [14-15]. Similarly, binding distance refers to the shortest distance between the adsorbate and the adsorbent [15]. A detailed analysis of these two aspects is discussed in Table 3. From the table, it is evident that the adsorption energies for both systems were negative, suggesting a favourable adsorption process. However, in the case of the propane-adsorbed system, it was more negative than that of butane, which implies better interaction between the considered sensing material and the gas/vapor. The obtained results were also compared with other sensing materials, and it was observed that Au-doped graphene has higher negative adsorption energy and shorter binding distance than others.

Table 3. Comparison of gas sensing parameters (adsorption energies and binding distances) between the existing literatures and the Au-doped graphene sheet

Adsorbed System	Adsorption Energy (eV)	Binding Distance (Å)	References
Au doped graphene + Propane	-1.074	2.473	Our work
Au-doped graphene + Butane	-0.926	2.500	Our work
Si-CNT + Propane	-0.441	-	[3]
S-doped Si-CNT + Propane	-3.144	3.071	[3]
Si-CNT + Butane	-3.014	-	[3]
S-doped Si-CNT + Butane	-3.016	3.011	[3]
epsilon phosphorene nanosheets + Butane (octa sites)	-0.766	-	[14]
epsilon phosphorene nanosheets + Butane (tetra sites)	-0.533	-	[14]
epsilon phosphorene nanosheets + Butane (top sites)	-0.547	-	[14]
epsilon phosphorene nanosheets + Propane (octa sites)	-0.723	-	[14]
epsilon phosphorene nanosheets + Propane (tetra sites)	-0.389	-	[14]
epsilon phosphorene nanosheets + Propane (top sites)	-0.376	-	[14]

4 Conclusion

The present research investigates the sensing ability of Au-doped graphene nanosheets toward propane and butane. In this study, several electronic properties such as HOMO-LUMO, MEP, and adsorption energy were analyzed for a detailed comparison. The stronger affinity between propane and the sensing material is demonstrated by the higher negative value of adsorption energy (1.15 times greater in magnitude) along with a shorter binding distance. From the HOMO-LUMO analysis, the energy gap was also found to be larger in the propane-adsorbed system (7.258 eV for alpha orbital, and 7.529 eV for beta orbital) than in the butane-adsorbed system (6.516 eV for alpha orbital, and 6.449 eV for beta orbital). The larger HOMO-LUMO gap in the propane-adsorbed system also denotes its stability. From the Raman and FTIR spectra, different vibrational characteristics of the gas-adsorbed Au-doped graphene were obtained. Both the structures showed increased current with rising bias voltage, indicating improved conductivity. Thus, the key observations suggest that Au-doped graphene nanosheet exhibits better interaction towards propane than butane, making it more promising for propane detection, which is crucial for LPG monitoring.

Acknowledgement

The authors are thankful to the Department of ECE, IEM Kolkata. The authors also acknowledge Mr. Indrajit Maity, Department of EE, IIT Bombay, for providing the necessary support. The authors also acknowledge Sayan Dey for his help.

References

1. M. Amarnath, A. Heiner, and K. Gurunathan, Highly sensitive room temperature liquefied petroleum gas sensor based on $CoSnO_2$ nanoislands deposited graphene layers. Synth. Met. **270**, 116607 (2020). https://doi.org/10.1016/j.synthmet.2020.116607.
2. M.S. B. Reddy, S. Kailasa, B. Geeta Rani, P. Munindra, K. Bikshalu, and K.V. Rao, CeO_2 nano-hexagons decorated rGO/CNT heterostructure for high-performance LPG sensing. SN Applied Sciences. **2**, 3 (2020). https://doi.org/10.1007/s42452-020-2220-7.
3. R.S. Singh, Sulfur-doped silicon carbide nanotube as a sensor for detecting liquefied petroleum gas at room temperature. Diam. Relat. Mater. **124**, 108932 (2022). https://doi.org/10.1016/j.diamond.2022.108932.
4. H. Rashid, A. Koel, and T. Rang, Simulations of propane and butane gas sensor based on pristine armchair graphene nanoribbon, in proceedings of the International Conference on Smart Engineering Materials (ICSEM), Bucharest, Romania, March 7-9 (2018). http://dx.doi.org/10.1088/1757-899X/362/1/012001.
5. M. Singla, and N. Jaggi, Enhanced hydrogen gas adsorption properties of B, N, and Au co-doped graphene in o-, m-, and p-configurations: DFT study. Diam. Rel. Mater. **127**, 109173 (2022). https://doi.org/10.1016/j.diamond.2022.109173.
6. I. Maity, S. Das, M. Gangopadhyay, and I. Maity, Understanding 2-propanol sensing mechanism of Pd modified graphene based gas sensor devices using DFT study, in proceedings of the 37th International Conference on VLSI Design and 23rd International Conference on Embedded Systems (VLSID), Kolkata, India, January 06-10 (2024). https://doi.org/10.1109/vlsid60093.2024.00011.
7. A. Roy, D. Mondal, and D. Jana, First-principles calculations of group-IV carbide quantum dots and single-layer heterojunctions with optical activity and short-wave infrared emission for efficient gas sensing. ACS Appl. Nano Mater. **8**, 4, 1852–1864, (2025). https://doi.org/10.1021/acsanm.4c06253.
8. A. Mahmood, T. Akram, and E.B. de Lima, Syntheses, spectroscopic investigation and electronic properties of two sulfonamide derivatives: A combined experimental and quantum chemical approach. J. Mol. Struct. **1108**, 496–507 (2016). https://doi.org/10.1016/j.molstruc.2015.12.039.
9. Y.M. Riza, Md. R. Parves, F.A. Tithi, and S. Alam, Quantum chemical calculation and binding modes of H1R; a combined study of molecular docking and DFT for suggesting therapeutically potent H1R antagonist. In Silico. Pharmacol. **7**, 1 (2019). https://doi.org/10.1007/s40203-019-0050-3.
10. Q. Fatima, H. Zhang, A.A. Haidry, R. Hussain, R.A. Alshgari, and S. Mohammad, Elucidating the optoelectronic properties Ag, Au and Pd doped graphene oxide using a DFT approach. Diam. Relat. Mater. **146,** 111151 (2024). https://doi.org/10.1016/j.diamond.2024.111151.
11. M. Roksana, S. Drewniak, T. Pustelny, M. Chrubasik, and G. Gryglewicz, Characterization of graphite oxide and reduced graphene oxide obtained from different graphite precursors and oxidized by different methods using Raman spectroscopy. Materials. **11**, 7, 1050 (2018). https://doi.org/10.3390/ma11071050.

12. A. I. Atyaa, N. D. Radhy, and L. S. Jasim, Synthesis and characterization of graphene oxide/hydrogel composites and their applications to adsorptive removal congo red from aqueous solution. J. Phys. Conf. Ser. **1234**, 1, 012095 (2019). https://doi.org/10.1088/1742-6596/1234/1/012095.
13. N. Lim, H. Kim, Y. Pak, and Y. T. Byun, Enhanced NO_2 sensing performance of graphene with thermally induced defects. Materials. **14**, 9, 2347 (2021). https://doi.org/10.3390/ma14092347.
14. V. Nagarajan and R. Chandiramouli, Sensing ability of liquefied petroleum gas by epsilon phosphorene nanosheets- a DFT investigation. J. Mater. NanoSci. **9,** 2, (2022). https://pubs.thesciencein.org/journal/index.php/jmns/article/view/285.
15. I. Maity, K. Ghosh, H. Rahaman, and P. Bhattacharyya, Selectivity tuning of graphene oxide-based reliable gas sensor devices by tailoring the oxygen functional groups: A DFT study-based approach. IEEE Trans. Device Mater. Rel. **17**, 4, 738-745 (2017). https://doi.org/10.1109/TDMR.2017.2766291.